EFFICIENT METHOD OF HARMONIC ANALYSIS OF THREE-PHASE CIRCUITS WITH NONLINEAR CONTROLLED SWITCHING ELEMENTS

CLAUDIU TUFAN[1], IOSIF VASILE NEMOIANU[2], MIHAI MARICARU[2], MARILENA STANCULESCU[2],
MIHAI EUGEN MARIN[2]

We devote our present study to the use of the Hănțilă method for solving three-phase circuits comprising nonlinear controlled switching elements (for example: thyristors). The method consists in replacing nonlinear circuit elements with controlled generators, comprising dependent sources and internal resistances. The value of these sources is determined using an algorithm with assured convergence, based on the construction of a Picard-Banach sequence, featuring successive passages between frequency domain and time domain, and *vice-versa*. The internal resistance value is chosen such that the algorithm convergence is ensured. The obtained results are compared for validation with those obtained by solving the circuit in time domain utilizing the LTspice software. Being a frequency analysis, it also considers the occurrence of the Gibbs phenomenon.

1. INTRODUCTION

Current trends in electricity consumption and production are leading to an increase in the number of nonlinear loads present in electricity networks [1–3]. The lack of concrete measures leads to the increasing pollution of the energy system with unwanted harmonics. The existence of harmonics cause: additional losses, heating, damage and can shorten the life of other equipment in the network. In most cases, increasing the immunity to harmonics leads to additional costs. For this reason, network operators are increasingly raising the issue of penalizing the distorted regime that occurs in electricity networks.

To reduce the presence of existing harmonics affecting the networks, several solutions have been developed: filters (active, passive or hybrid), oversizing of equipment and conductors, reconfiguration of networks, re-wiring the elements in the given circuit, etc. All these measures are quite expensive and come with a high cost of implementation. Therefore, one must take corrective measures from the design phase of equipment and networks. To evaluate the effectiveness of these measures it is useful to make an analysis of the resulting distorted regime.

An important role is played by the computation methods that can determine the distorted effect of nonlinear loads and allow the adoption of remedial solutions. Methods and software for the analysis of circuits with nonlinear elements have been developed. The main methods propose solving the circuit in time domain, in frequency domain or are combinations between the two. The existing methods have certain advantages, disadvantages or limitations which are described in detail in the literature.

The use of the Hănțilă method [4] for solving three-phase circuits with nonlinear resistors is comprehensively illustrated in [5], in the case of different reactances presented by the symmetrical components. The method consists in developing an algorithm with assured convergence, based on the construction of a Picard-Banach sequence, with successive iterative transitions from the frequency domain to the time domain and *vice-versa*. The method was proposed for solving circuits with nonlinear elements in [4] and was later developed

in [6–8]. Its application in three-phase circuits was suggested in [9] and it was analyzed in the case of concrete examples in [5]. The results were compared for validation with those obtained by solving in the time domain with LTspice [10]. Unfortunately, LTspice software does not have the capability of analyzing three-phase circuits presenting different reactances on symmetrical sequences. The software treats the three-phase circuit as an ordinary circuit, in time domain, without the possibility of reducing the computation effort by analyzing a single-phase, as proposed in [5]. Although benefitting from the absence of the Gibbs effect, we also mention that in time domain the circuits presenting time-constants greater than $T = 20$ ms, may add to the computation burden in terms of algorithm complexity and thus in running time duration. Greater time-constants account for the presence within the circuit of large inductances and capacitances, as presented in more detail in [11].

The Hănțilă method has been successfully used in solving other electrical engineering problems: the computation of the stationary magnetic field, or the electromagnetic field in nonlinear media [12]. Even if it uses complex demonstrations and advanced knowledge of functional analysis (Hilbert spaces, Picard-Banach sequences, contractions, non-expansive functions, fixed points, Lipschitz functions, uniformly monotone functions, etc.), the method can be easily applied and simulated using the computer [5].

The purpose of this paper is to analyze the use of the Hănțilă method for solving three-phase circuits with nonlinear controlled switching elements (as in the case of thyristors). Nonlinear resistors with controlled switching are more and more common in modern equipment. The operating principle of the active filters is also based on this switching possibility.

To prove the validity of the approach, the obtained results are compared with those resulted by solving the circuit in time domain utilizing the LTspice software package.

2. APPLICATION OF THE HĂNȚILĂ METHOD FOR SOLVING CIRCUITS CONTAINING NONLINEAR CONTROLLED SWITCHING ELEMENTS

In this section, we present in detail the application of the

---
[1] Electrical Engineering Doctoral School, University POLITEHNICA of Bucharest, E-mail: claudiu.tufan@stud.electro.pub.ro
[2] Electrical Engineering Department, University POLITEHNICA of Bucharest, E-mail: iosif.nemoianu@upb.ro

Hănțilă method using the voltage correction of the equivalent source. The method can similarly be applied using current correction, the two variants of the method being dual [5, 9].

In the case of nonlinear elements with time-controlled switching, the current is a function of voltage and time [5]. In fact, there are two characteristics that are switched in the time domain when the command appears ($t = t_\alpha$), and back when a threshold condition for the current or voltage at the terminals is not satisfied. The application of the Hănțilă method is similar to [5, 9].

In what follows, we underline only the differences from the implementations presented in [5, 9], namely those determined by this switching of the characteristics in the time domain, without repeating the parts that remain valid. The characteristic of such a nonlinear element with time-controlled switching is of the form:

$$i = f(u, t_\alpha),\qquad(1)$$

where i and u are the current and the voltage of the nonlinear element. The relationship (1) represents the family of the two characteristics corresponding to t_α – for the thyristor case.

As in [5], the nonlinear elements with the characteristic given in (1) are replaced by voltage generators consisting of voltage sources e, nonlinearly controlled, and internal resistances R:

$$u = R \cdot i + e,\qquad(2)$$

with

$$e = u - Rf(u, t_\alpha) = g(u, t_\alpha).\qquad(3)$$

According to [4, 5, 12], one chooses R such that $g(u, t_\alpha)$ be a contraction in the Hilbert space corresponding to the periodic functions (of period T), such that there is $q \in [0,1)$, satisfying the inequality:

$$\|g(u_1, t_\alpha) - g(u_2, t_\alpha)\| \le q\|u_1 - u_2\|,\qquad(4)$$

for each u_1, u_2.

If (4) is verified for $q = 1$, then $g(u, t_\alpha)$ is non-expansive.

In this way, we defined the function $g(u, t_\alpha)$ performing the transition in time domain from u – the voltage at the terminals of the nonlinear element, to the voltage source e, nonlinearly controlled, and we made sure that it is a contraction, having the contraction factor q. The function $g(u, t_\alpha)$ ensures the correction in time domain with the characteristic of the nonlinear element. Starting from the characteristic function f, which depends in this case also on t_α, we defined $g(u, t_\alpha)$ that implicitly depends on t_α. The fact that it also depends on t_α does not prevent its contractive nature, if f is a Lipschitz function and piecewise uniformly monotonous [6–9]. In general, in the operation range, the characteristics of the nonlinear elements are described by functions having such properties. The switching moment can lead to Gibbs phenomenon (due to Fourier series truncation), subject that will be treated in the next section dedicated to an illustrative example.

For the nonlinear one-port element, R must be chosen in the interval $(0, 2/\Lambda)$ to ensure that $g(u, t_\alpha)$ is a contraction, where Λ is the Lipschitz constant corresponding to the function $f(u, t_\alpha)$ [7, 9].

Using the above-presented replacement of the nonlinear loads with nonlinear controlled generators, one obtains a linear circuit in periodic regime. The computation on a single phase, on sequences, has been presented in [5]: after computation, one defines the function of complex variable $h(\underline{E})$, by which the complex voltage $\underline{U}$ is obtained at the terminals of the nonlinear element, due to the source of the nonlinear element having the complex electromotive force $\underline{E}$ [5]:

$$\underline{U}_k = (\underline{E}_k + \underline{E}_{gk})\underline{Z}_{ek}/(\underline{Z}_{ek} + R) = h_k(\underline{E}_k),\qquad(5)$$

where $\underline{U}_k$ is the voltage at the terminals of the nonlinear element, $\underline{E}_k$ is complex voltage of the of the nonlinear controlled emf, $\underline{Z}_{ek}$ and $\underline{E}_{gk}$, being the impedance, and the source of the equivalent generator connected to the nonlinear element's terminals, for each harmonic of order k and each symmetrical component.

In frequency domain, the function $h(\underline{E})$ ensures the correction according with the circuit connected to the terminals of the nonlinear element, being always non-expansive, since always $R \ge 0$, [5]:

$$\underline{U'}_k - \underline{U''}_k = \frac{(\underline{E'}_k + \underline{E''}_k)\underline{Z}_{ek}}{\underline{Z}_{ek} + R} = h_k(\underline{E'}_k) - h_k(\underline{E''}_k).\qquad(6)$$

Using the above-defined functions, $g(u, t_\alpha)$ – contractive and $h(\underline{E})$ – non-expansive, the following correspondences may be highlighted:

$$u \xrightarrow{g(t_\alpha)} e \quad \text{in time domain and}\qquad(7)$$

$$\underline{E} \xrightarrow{h} \underline{U} \quad \text{in frequency domain.}\qquad(8)$$

In the Hilbert space corresponding to the periodic functions (of period T), one can construct a Picard-Banach series, based on the following iterative process, with successive transformations from the frequency-domain to the time-domain, and reciprocally (presented from iteration n to iteration $n+1$, maintaining the above notations) [5, 9]:

$$e^{(n)} \xrightarrow{F} \underline{E}^{(n)} \xrightarrow{h} \underline{U}^{(n)} \xrightarrow{F^{-1}} u^{(n)} \xrightarrow{g(t_\alpha)} e^{(n+1)},\ (9)$$

where F is the Fourier transform, and F^{-1} is the inverse Fourier transform.

The statement and justifications of [5] are maintained: the iterative process consists of a composition between a contraction and some non-expansive functions. The process is a contraction and is convergent in both frequency and time domains. The convergence is always ensured, as long as R is chosen according with (4).

The correction imposed by the nonlinear characteristic with controlled switching, takes place only in time-domain, and can be easily implemented in the computation software.

Using the value of the nonlinear controlled source, computed with a good enough precision, one can compute in frequency domain the currents and the voltages for all circuit elements [5].

3. ILLUSTRATIVE EXAMPLE

We propose the computation of the circuit given in Fig. 1, consisting of a controlled rectifier powered by a three-phase symmetrical generator with neutral. Our choice for this type of circuit was justified by the fact that we expected it to generate all kinds of harmonics, including multiple of 2 and 3 ones. The following characteristics of the circuit elements have been considered: three-phase sinusoidal generator, with

symmetrical sources of amplitude 325 V and frequency 50 Hz, $R_l = 1\Omega$, $R_s = 25\ \Omega$, $R_2 = 10\ \Omega$, $L_l = 2\times10^{-4}\,\text{H}$, $L_s = 4\times10^{-2}\,\text{H}$.

As presented in [5], because the circuit analysis is performed in frequency domain, the Hănțilă method can be used with any values of circuit elements on sequences or harmonics. It is therefore very useful, for example, in the case of generators presenting different reactances on sequences. In the illustrative example, we will use circuit elements with the same values on different sequences, to be able to compare the results against those provided by LTspice (which does not have the possibility to solve the circuit considering different reactances on sequences).

We will use for the thyristor *Th* the piecewise linearized characteristic presented in Fig. 2. The method allows also to use other types of characteristics.

period T, is given by:

$$i = f(u,t_\alpha) = \begin{cases} uG_c + V_f(G_b - G_c), t \in \begin{cases}[t_\alpha, t_b) \text{ if } t_b < T \\ [0, t_b) \cup [t_\alpha, T] \text{ if } t_\alpha > t_b, \end{cases} \\ uG_b \text{ for the rest of the period } T \end{cases}$$

(10)

where t_b is the blocking time for which the condition $u < V_f$ is fulfilled for the first time after the gate control signal disappears (Fig. 3). The inequality $t_\alpha > t_b$ appears when the conduction started in the previous period, and it is maintained in the current period until fulfilling the condition $u < V_f$. For the thyristor *Th* of Fig. 1 we have: the blocking resistance $R_b = 1/G_b = 10^4\,\Omega$, the conduction resistance $R_c = 1/G_c = 10^{-4}\,\Omega$, $V_f = 1\,\text{V}$ and we choose $t_\alpha = T/4 = 0.005$ s.

Fig. 1 –Three-phase circuit proposed for computation.
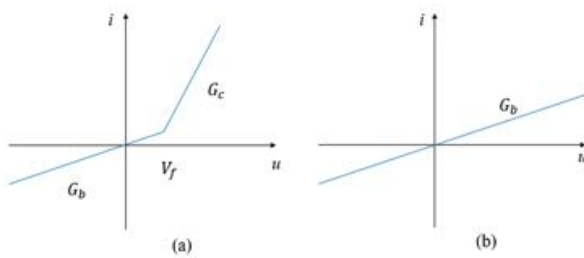
Fig. 2 – The thyristor piecewise linearized characteristic: (a) with signal on the gate (b) without signal on the gate.

The characteristic of Fig. 2a is valid for the time interval corresponding to the apparition of the control signal on the gate until the voltage u drops under a threshold value V_f. It is characterized by the blocking conductance G_b if $u < V_f$ or conduction G_c if $u \geq V_f$, respectively. The characteristic shown in Fig. 2b is valid before applying the control signal to the gate and after the voltage u dropping under the threshold value V_f, being characterized only by the blocking conductance G_b.

In this case, the characteristic function form (1), for a

4. COMPUTATION USING THE HĂNȚILĂ METHOD

We use the Hănțilă method with voltage correction of the nonlinear load corresponding source. From (3), the function $g(u,t_\alpha)$ becomes:

$$e = g(u,t_\alpha) = \begin{cases} u\left(1 - \dfrac{R}{R_c}\right) - \dfrac{RV_f(R_c - R_b)}{R_b R_c}, t \in \begin{cases}[t_\alpha, t_b) \text{ if } t_b < T \\ [0, t_b) \cup [t_\alpha, T] \text{ if } t_\alpha > t_b. \end{cases} \\ u\left(1 - \dfrac{R}{R_b}\right) \text{ for the rest of the period } T \end{cases}$$

(11)

To ensure that $g(u,t_\alpha)$ is a contraction, R must be chosen in the interval $(0,\ 2\cdot R_c)$. A greater value for R ensures a better contraction factor and a superior convergence speed.

(a)

(b)
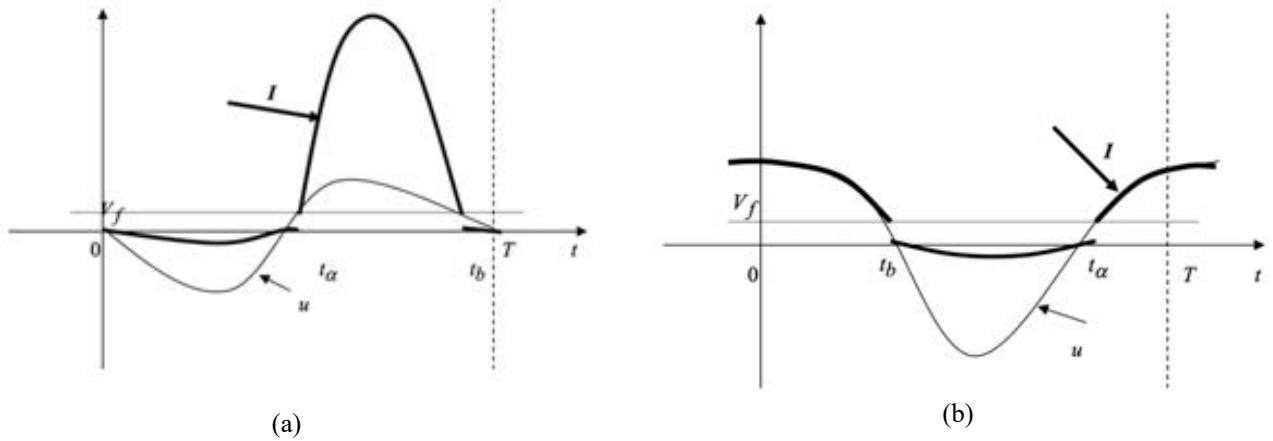
Fig. 3–Thyristor current and voltage graphs for: (a) $t \in [t_\alpha, t_b)$ if $t_b < T$ and (b) $t \in [0, t_b) \cup [t_\alpha, T]$ if $t_\alpha > t_b$.

If we choose $R = R_c$, it results:

$$e = g(u, t_\alpha) = \begin{cases} \dfrac{V_f(R_b - R_c)}{R_b}, t \in \begin{cases} [t_\alpha, t_b) \text{ if } t_b < T \\ [0, t_b) \cup [t_\alpha, T] \text{ if } t_\alpha > t_b \end{cases} \\ u\left(\dfrac{R_b - R_c}{R_b}\right) \text{ for the rest of the period } T \end{cases}$$

(12)

To perform the simulation, we used a classical algorithm to calculate the coefficients of the Fourier series, respectively of the inverse Fourier transform. Using the existing FFT routine in GNU Octave [14] did not give satisfactory results: large computational errors propagate to the repeated transitions between the time domain and the frequency domain, and even if the time required for a single iteration is very short, the number of iterations increases significantly. An amplification of the Gibbs phenomenon was observed.

To compute the coefficients of the Fourier transform, we proceed as follows: we split he period T in a number of equal intervals Δt; we considered the linear approximation of the function $e(t)$ between each pair of points t_n and t_{n+1}, and computed the integrals

$$\int_{t_n}^{t_{n+1}} \sin(k\omega t) \cdot (a_n t + b_n) dt ,$$

respectively

$$\int_{t_n}^{t_{n+1}} \cos(k\omega t) \cdot (a_n t + b_n) dt .$$

We reduced to the first quadrant the arguments for $\sin(k\omega t)$ and $\cos(k\omega t)$ to compute F and F^{-1} to decrease the floating-point computation errors. Other computational algorithms used for the Fourier transform may prove more efficient and, possibly, allow for a shorter computational time.

In the controlled operation regime, by switching between the characteristics, at t_α a signal jump appears, situation multiplied three times in the case of a three-phase scheme. The rapid voltage variation at the terminals of the thyristor accentuates the manifestation of the Gibbs phenomenon. We analyze the possibility of implementing a solution for its reduction by retaining several harmonics used in the truncation equal to the number of equidistant time-points used for sampling.

The Fourier series is truncated by retaining the first 6000

harmonics and the period T is also divided to 6000 equidistant points. The iterations stops when the distance (the error) computed for the voltage source value corresponding to two successive iterations (defined according to [5, 13]) is less than 10^{-6} V. The computation algorithm was implemented using GNU Octave 6.2.0 [14].

(a)

(b)
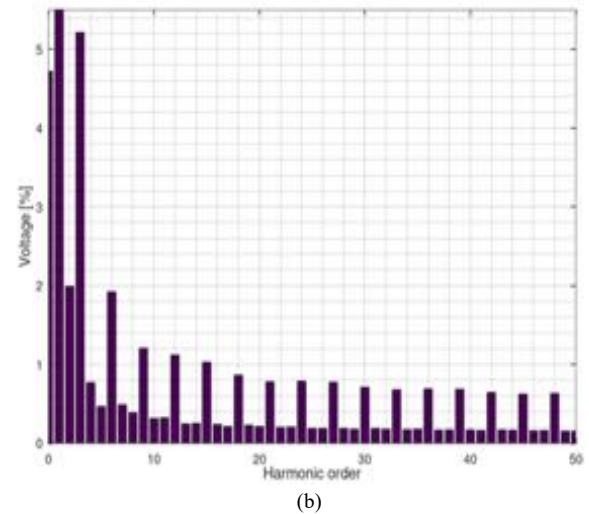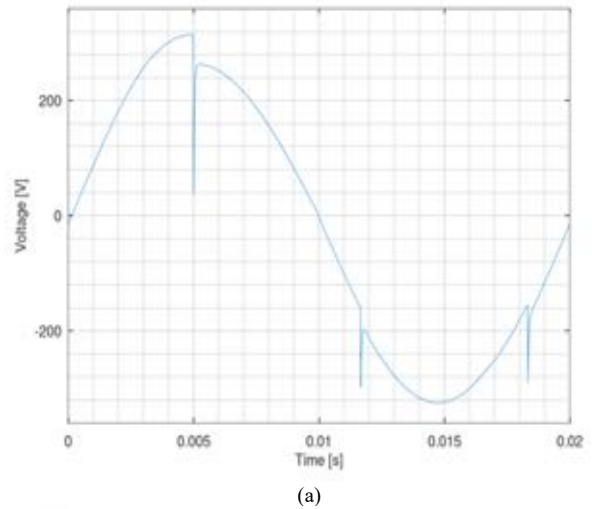
Fig. 4 –The voltage on $Th + R_2$: (a) in time-domain (b) detail of the harmonic spectrum up to 50th harmonic order.

Once the nonlinearly controlled voltage source with the desired error has been calculated, the currents and voltages

can be calculated for all circuit elements [5 9]. Figure 4a shows the voltage on $Th + R_2$, and in Fig 4b is given a detail of its harmonic spectrum up to rank 50, presented as a percentage of the fundamental. The absence of the Gibbs phenomenon is observed.

Figure 5 shows the current computed for the main branches of the circuit: Fig. 5a the current though the thyristor *Th* (with the detail of Fig. 5b and c), the current through the load resistance R_s (Fig. 5d), the current though the generator (Fig. 5e), and in Fig. 5f the current through the neutral.
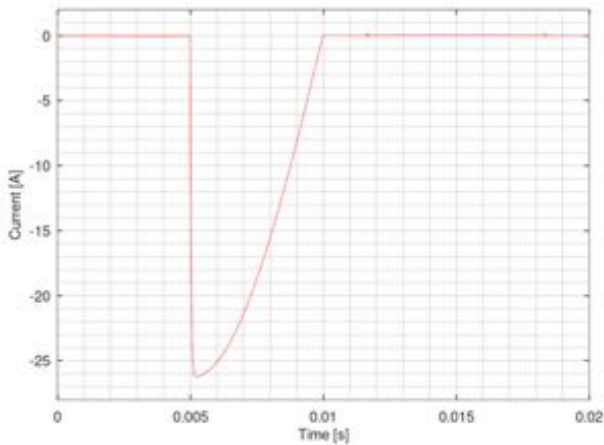
(a)
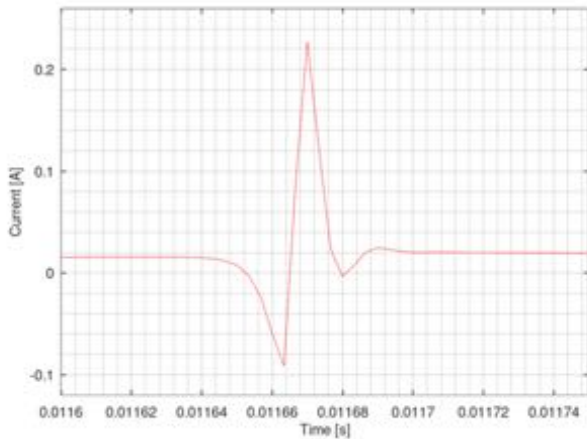
(b)
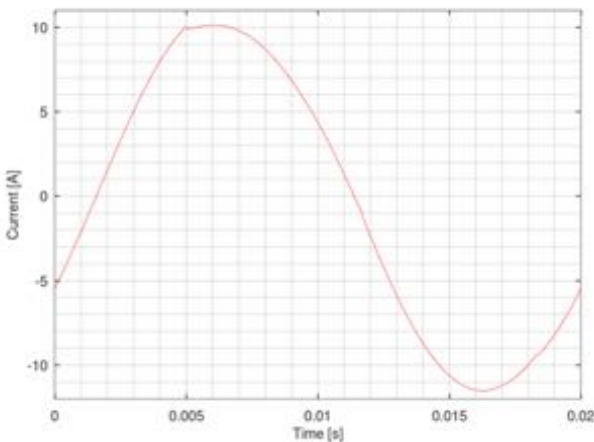
(c)

In Fig. 5a, with the detail from 5b, it can be observed a synthesis error for the current through the thyristor in the discontinuity points on the other 2 phases. Similarly, the effect occurs, but to a lesser extent, at the point of return from

conduction to blockage for phase 1. The same is true for the currents in Fig. 5c and d.

Even if it is not visible in the voltage graph, the Gibbs phenomenon is being felt in the current graphs. By increasing the number of harmonics (maintaining the equality with the number of sampling points), the amplitude of the error decreases.
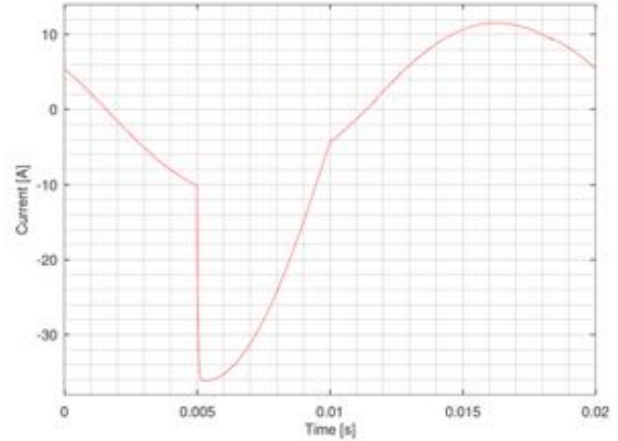
(d)
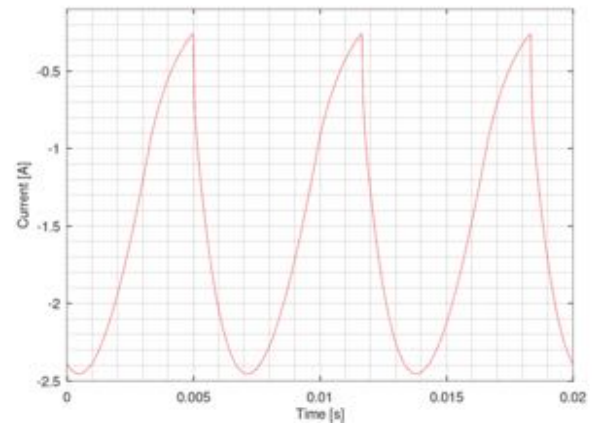
(e)
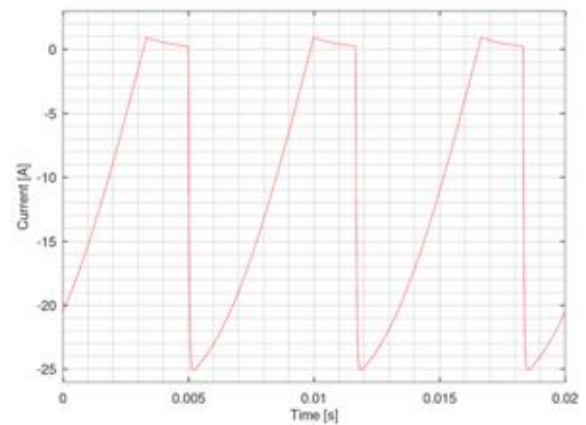
(f)

Fig. 5 – Current variation in time-domain through: (a) *Th* with the detail in (b), (c) R_s, (d) the generator e_{ga}, (e) neutral between the wye generators and wye thyristors (f) neutral between wye thyristors and wye linear loads.

5. COMPARATIVE STUDY

In this subsection, we compare the results obtained by the Hănțilă method, for different numbers of harmonics, and different sampling points (with the same stopping criterion 10^{-6} V). The results are compared to the ones obtained using

LTspice version 17.0.31.

Like [5], an increase (by successive increments) of the maximum distance (error) from the fixed point of the Picard-Banach series can be calculated when applying the Hănțilă method, for the calculation of the controlled voltage source. The distance is obtained from the result that can be obtained with the chosen calculation parameters, discussed above. As expected, different parameters mean different fixed points. We present the distances for the 3 proposed models.

Table 1

The distances for the three proposed models.

Simulation	No. of harmonics	No. of sampling points	Distance
1	6000	6000	9.57×10^{-4} V
2	1000	6000	4.04×10^{-4} V
3	1000	1000	3.68×10^{-4} V

The simulation of the circuit in LTspice used to model thyristors as voltage controlled current sources (arbitrary behavioral current source). LTspice software was chosen due to its wide acceptance and recognition among professionals, providing thus an easy to use and versatile tool for re-modeling the presented circuit.

The comparison with LTspice takes place in time-domain: visually by overlapping the results and calculating a 2nd-order norm of the differences between the values obtained by LTspice and the values calculated at the same time points using the Hănțilă method. Thus, we have

$$\varepsilon_{dif} = \sqrt{\frac{\sum \Delta U_n^2 \cdot \Delta t_n}{T}}, \quad (13)$$
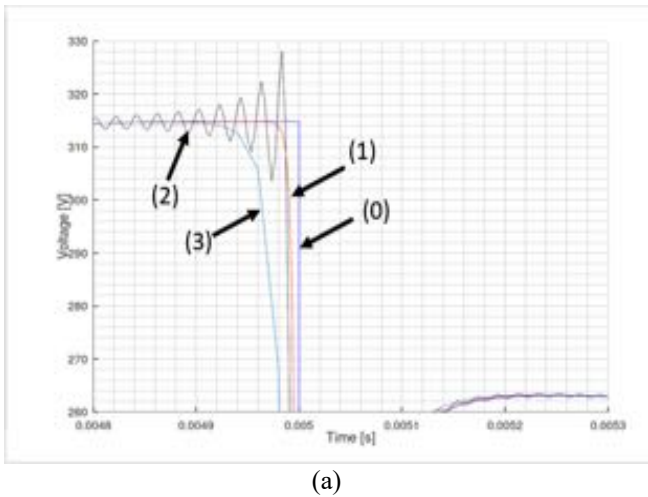
We obtained the following values of the norm ε_{dif} for the three simulated variants, compared to LTspice for the voltage on $Th + R_2$:

Table 2

The norm ε_{dif} for the three simulated variants, compared to LTspice for

the voltage on $Th + R_2$.

Simulation	No. of harmonics	No. of sampling points	ε_{dif}
1	6000	6000	2.72 V
2	1000	6000	3.70 V
3	1000	1000	5.75 V

Figure 6 presents two details regarding the overlap of the results obtained in the time-domain for the voltage on $Th + R_2$, around the jump points, the place where the big differences between the results appear.

In Simulations 1 and 3, the Gibbs phenomenon is imperceptible, while it is very accentuated in Simulation 2. It is observed that a higher number of harmonics, respectively of sampling points give a more accurate result. Even if it is visibly affected by the Gibbs phenomenon, Simulation 2 has, on average, values closer to the result obtained with LTspice than Simulation 1. For Simulation 3, the time was sampled with the same duration of 2×10^{-5} s. For the Simulations 1 and 2, time was sampled using an interval of 3.33×10^{-6} s, values much higher than the time step of 10^{-14} s reached by the simulation in the time domain. A significant increase in the number of points, correlated with the same number of harmonics, would lead to a result very close to that obtained with LTspice, but would significantly increase the time and computation effort.

(a)   (b)
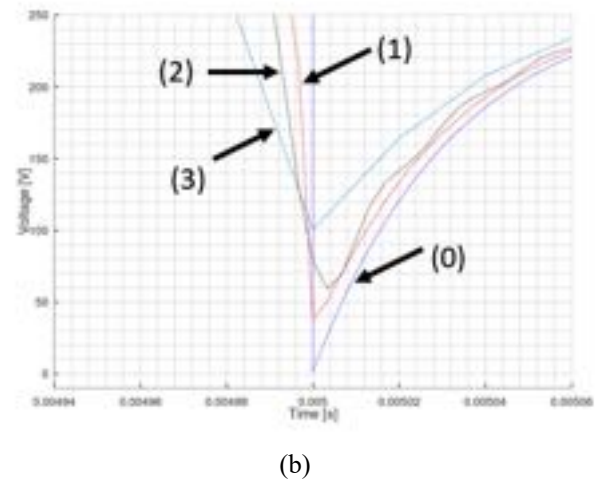
Fig. 6 – The voltage on $Th + R_2$ for the four simulations: LTspice **(0)**, Simulation 1 **(1)**, Simulation 2 **(2)** and Simulation 3 **(3)**, with the details: (a) and (b).

where ΔU_n is the difference between the values of the voltage obtained using Ltspice and Hănțilă method, respectively, at point n, and Δt_n is the time step (between the point n and $n+1$) used by LTspice.

In LTspice a transient analysis is performed, were the time step value is automatically lowered in the case of fast transitions. During the simulation a minimum value for the time step of 10^{-14} s is observed. For this reason, we introduced Δt_n, for the computation of the norm; in this case Δt_n is variable.

From the performed simulations, it results that the reduction of the Gibbs phenomenon is maintained if the number of sampled calculation points is in the range +/– 10 % compared to the number of harmonics considered at truncation.

The actual nonlinear features are smoother and have less abrupt variations than the linearized model considered in this illustrative example. We expect a sufficiently accurate result in such situations using truncation to a smaller number of harmonics.

Solving the proposed model using LTspice was not an

easy task. Several adjustments to the values of the circuit elements were required, and the initial time step had to be guessed. In all previous attempts, the software returns the error that the time step is too small, and the solution is not possible. In fact, we considered a circuit that we finally managed to solve with LTspice, and we also solved it using the Hănțilă method and not the other way around.

Also, as mentioned in [5], LTspice using time-domain computation cannot solve the circuits with different reactances on sequences and is not useful in such applications.

The comparison with LTspice reconfirms that the solution obtained by using Hănțilă method is correct and converges to the correct result.

As further development the target is to identify compatible computational algorithms, more efficient (in terms of speed and accuracy) and with non-uniform sampling capabilities (namely thickening of computational points in the time-domain around the signal jump areas, to reduce the computational effort), for both direct and inverse Fourier transforms.

Once the voltages and currents in the frequency domain have been calculated, the calculation of the powers can be done very easily, as well as the transfer of power on harmonics, as shown in [5]. In this case, the principles already stated are maintained: the generator delivers complex power on the fundamentals. Nonlinear loads consume power on the fundamentals. Part of this power is absorbed internally, and the rest is "delivered" on harmonics. Tellegen's theorem, that ensures the conservation of powers is proven, as well as the Țugulea theory regarding the power flow within three-phase networks and its subsequent developments, is also confirmed [15–17].

6. CONCLUSIONS

The Hănțilă method is a useful computation tool for solving three-phase circuits with nonlinear elements, which can easily highlight the distorting effect. Since the correction with nonlinear characteristics is made in the time-domain, the method can be easily applied in the case of nonlinear loads with time-controlled switching or composed of several piecewise defined characteristics. The circuit analysis being made in the frequency-domain, the method allows the introduction in the calculation of the elements with different values (reactances or resistances) on harmonics or sequences (an advantage compared to the solution in the time-domain). The method can be easily used from the sizing and design phase of both circuits and power networks, to highlight and consider the distorting effects as well as the transfer of power on harmonics, for each circuit element, the nonlinear ones included. For the latter, the method puts in evidence the direction of the powers exchanged on harmonics – absorbed *vs.* generated. The so obtained balance of powers verifies Tellegen's theorem and confirms Professor Țugulea's theory and its subsequent developments [15–17], concerning power flow in three-phase networks containing nonlinear elements [5]. This feature is important for an optimal implementation and verification of possible corrective measures. The method brings a dramatic reduction of the computation burden, as it allows solving the circuit on a single phase.

Although it is based on complex demonstrations and requires advanced knowledge of functional analysis, the method remains easy to understand, apply and simulate on the computer.

The results obtained using the Hănțilă method are validated by those obtained with LTspice in the time-domain. The method can be used even when the time solution is not possible due to the need of choosing a very short time step.

In the simulation of circuits using the Hănțilă method, the Gibbs phenomenon can be significantly reduced by maintaining a ratio of 1 (+/– 10 %) between the number of computation points and the number of harmonics used to truncate the Fourier series.

As a direction of further development of the method, an important objective is to use of more efficient algorithms for the calculation of direct and inverse Fourier transforms, including non-uniform sampling in the time-domain.

REFERENCES

1. M. Gavrilas, R. Toma, *Flexible alternating current transmission system optimization in the context of large disturbance voltage stability*, Rev. Roum. Sci. Techn. Électrotechn. et Énerg., **66**, *1*, pp. 21–26 (2021).
2. P. Kumar, M. Kumar, N. Pal, *An efficient control approach of voltage and frequency regulation in an autonomous microgrid*, Rev. Roum. Sci. Techn. Électrotechn. et Énerg., **66**, *1*, pp. 33–39 (2021).
3. B. Ali, A.A. Khan, *Real-time distribution system analysis and load management algorithm for minimizing harmonics*, Rev. Roum. Sci. Techn. Électrotechn. et Énerg., **66**, *4*, pp. 237–242 (2021).
4. I.F. Hantila, *A method for solving nonlinear resistive networks,* Rev. Roum. Sci. Techn. Électrotechn. et Énerg., **24**, *2*, pp. 217–226 (1979).
5. C. Tufan, I.V. Nemoianu, *Method for the Analysis of Three-Phase Networks Containing Nonlinear Circuit Elements in View of an Efficient Power Flow Computation*, Electronics, **10**, *21*, pp. 1–19 (2021).
6. I.F. Hantila, M. Maricaru, R.M. Ciuceanu, L. Corlan, *Harmonic analysis of circuits with nonlinear resistive elements*, Rev. Roum. Sci. Techn. Électrotechn. et Énerg., **57**, *4*, pp. 333–340 (2012).
7. G.M. Vasilescu, I.F. Hantila, M. Maricaru, I. Barsan, V. Stanciu, *A new method for solving the periodic steady state of nonlinear circuits*, Rev. Roum. Sci. Techn. Électrotechn. et Énerg., **59**, *4*, pp. 339–349 (2014).
8. I.F. Hantila, F. Constantinescu, A.G. Gheorghe, M. Nițescu, M. Maricaru, *A new algorithm for frequency domain analysis of nonlinear circuits*, Rev. Roum. Sci. Techn. Électrotechn. et Énerg., **54**, *1*, pp. 57–66 (2009).
9. I.F. Hantila, M. Maricaru, M. Stanculescu, G.M. Vasilescu, *Method for analyzing three-phase networks with nonlinear resistive elements*, Rev. Roum. Sci. Techn. Électrotechn. et Énerg., **64**, *2*, pp. 103–106 (2019).
10. Analog Devices, https://www.analog.com/en/design-center/design-tools-and-calculators/ltspice-simulator.html [accessed: March 12, 2022].
11. F. Constantinescu, A.G. Gheorghe, M.E. Marin, G. Vătăşelu, V. Ştefănescu, D. Bodescu, *New models for frequency domain simulation of home appliances networks*, Proceedings of the 11th International Symposium on Advanced Topics in Electrical Engineering, Bucharest, Romania, 28–30 March 2019.
12. G.M. Vasilescu, M. Maricaru, *An efficient procedure for solving non-linear problems in electrical engineering: Hantila Method*, Rev. Roum. Sci. Techn. Électrotechn. et Énerg., **64**, *2*, pp. 187–194 (2019).
13. I.F. Hantila, N. Vasile, E. Demeter, S. Marinescu, M. Covrig, *Câmpul electromagnetic staționar în medii neliniare*, ICPE, București, Romania, 1998, pp. 46–51.
14. J. W. Eaton, https://www.gnu.org/software/octave/ [accessed: March 12, 2022].
15. I.V. Nemoianu, M.I. Dascalu, V. Manescu (Paltanea), G. Paltanea, R.M. Ciuceanu, *In-deep First Assessment of the Influence of Nonlinear Elements in Three-Phase Networks with Neutral*, 11th International Symposium on Advanced Topics in Electrical Engineering (ATEE),

28–30 March 2019.

16. I.V. Nemoianu, M.I. Dascalu, V. Manescu (Paltanea), G. Paltanea, A. Radulian, *Detailed evaluation for the power flow effects of nonlinear circuit elements in three-phase networks without neutral*, Rev. Roum. Sci. Techn. Électrotechn. et Énerg., **64**, *3*, pp. 195–198 (2019).

17. I.V. Nemoianu, V. Manescu (Paltanea), G. Paltanea, R.M. Ciuceanu, *Insight into the Non-Symmetry and Residual Active and Reactive Power Flow in the case of Three-Phase Distorting Networks without Neutral*, 12th International Symposium on Advanced Topics in Electrical Engineering (ATEE), Bucharest, Romania, 25–27 March 2021.